CHEMICAL ENGINEERING TRANSACTIONS

VOL. 118, 2025

A publication of AIDIC
The Italian Association of Chemical Engineering
Online at www.cetjournal.it

Guest Editors: Laura Piazza, Francesco Donsì, Giorgia Spigno, Paolo Ciambelli, Luca di Palma
Copyright © 2025, AIDIC Servizi S.r.l.
ISBN 979-12-81206-19-9; **ISSN** 2283-9216

DOI: 10.3303/CET25118004

Preliminary Step of the Digital Twin Model Design for High Moisture Extrusion of Proteins from Alternative Sources

Gianfranco Di Lorenzo*, Donatella Albanese, Francesco Marra

Industrial Engineering Department, University of Salerno, Fisciano (SA), Campania 84084, Italy.
gdilorenzo@unisa.it

The objective of this study is to develop a deeper understanding of the high-moisture extrusion (HME) process for producing meat-like products from alternative proteins and to establish a foundation for the implementation of a Digital Twin (DT) framework. Since twin screw extruder (TSE) is largely a black-box system with limited temperature sampling and no direct velocity measurements, a mechanistic modelling framework was developed as an initial step toward DT implementation. To achieve this, numerical simulations were conducted to analyse key transport phenomena and axial velocity distribution, pumping efficiency, and dispersive mixing behaviour, within a co-rotating twin screw extruder. A steady-state approximation with frozen rotor analysis was employed to model TSE behaviour. The numerical simulations provided insights into the axial velocity distribution along the screws, the effect of screw speed on pumping efficiency, and the role of dispersive mixing in the process. These findings contribute to a better understanding of the extrusion process and lay the groundwork for future advancements in DT applications, aiming at process optimization, improved material structuring, and enhanced production efficiency for alternative protein-based meat analogues.

1. Introduction

High-moisture extrusion processing has been used for years to transform plant-based proteins into fibrous, meat-like structures at 40-80% moisture, with an extended cooling die aiding fiber formation (Hong et al., 2022). To support this, the cooling zone must stay below 75 °C (Xiaonan et al., 2024). Moisture, screw, temperature, and pressure affect the material, but detecting changes is challenging. Numerical simulation helps reveal protein flow behavior (Dashu et al., 2024). With industrial digitalization and the rise of the Internet of Things, the Digital Twin concept has emerged as a tool for process management, though its first agrifood application is yet to be demonstrated (Verboven et al., 2020). A Digital Twin, simulating transport phenomena, enables live interaction between the physical and digital systems, allowing the machine to learn from real-world data to optimize process conditions and develop products with desired characteristics (Datta et al., 2022). This study aims to deepen understanding of high-moisture extrusion for meat-like products and lay the groundwork for a Digital Twin framework by developing a mechanistic modeling approach to simulate transport phenomena and flow behavior.

2. Material and methods

2.1 Design of co-rotating twin screw extruder

A lab-scale HME system was considered for mechanistic modeling framework design. HME system consisted of a parallel co-rotating TSE (L/D: 30 with a cross-sectional diameter of 13.4 mm) fitted with a liquid-cooled slot die (H x W x L : 44 x 77 x 270 mm) that leads the extrudate into a slab of rectangular section (H x W: 5 x 18 mm). Along the extruder, nine alternate heating cartridges (considering the power range of 0- 200 W for each cartridge), coupled with temperature sensors, allowed the control of the temperature profile along the extruder length. The pressure value was monitored at inlet of liquid-cooled slot die.

Screws of extrusion

As shown in Figure 1, the twin screw is comprised of the following elements:

Paper Received: 28 May 2025; Revised: 23 June 2025; Accepted: 30 August 2025
Please cite this article as: Di Lorenzo G., Albanese D., Marra F., 2025, Preliminary Step of the Digital Twin Model Design for High Moisture Extrusion of Proteins from Alternative Sources, Chemical Engineering Transactions, 118, 19-24 DOI:10.3303/CET25118004

- feeding zone composed of n.2 screw elements with 8 mm lead (8/13.4/0.53/R) and n.2 screw elements with 20 mm lead and 0.53 mm crest (20/13.4/0.53/R);
- transport zone composed of n.15 screw elements with 12 mm lead and 0.53 mm crest (12/13.4/0.53/R);
- mixing zone composed of kneading block with n.3 elements at 0° orientation (0°/13.4/K) and n.5 elements with 90° orientation (90°/13.4/K);
- extrusion zone composed of n.2 elements with 12 mm lead and 2 mm crest (12/13.4/2/R).

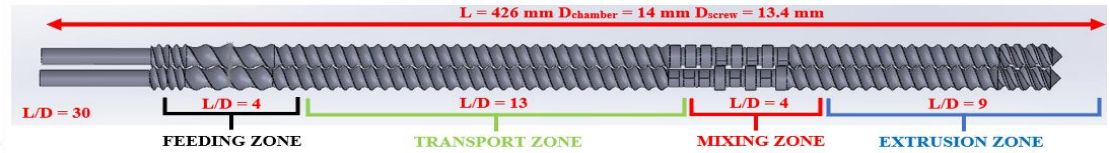

Figure 1 Screw configuration

2.2 Mathematical model development

The description of the problem under consideration must take into account the balances of momentum, energy and matter, with the additional term of viscous generation. The complexity of the problem lies in dealing with an intrinsically variable-domain system that was described with frozen rotor analysis. On Table 1, Eqs(1, 2 and 3) were used to determine the temperature distribution within the material processed along the extruder. Navier-Stokes and continuity equations (Eqs(4 and 5)) were coupled with Eqs(1, 2 and 3). In addition, gravity could be neglected as the Jeffrey-number (Kousemaker et al., 2024) – the ratio of gravity to viscous forces – is low.

Table 1 Transport phenomena equation used in mathematical model

Fourier equation	$\rho C_p \boldsymbol{u} \cdot \nabla T + \nabla \cdot (-k \nabla T) = Q_p + Q_{vd}$	(1)	Navier Stokes equation	$\rho (\boldsymbol{u} \cdot \nabla)\boldsymbol{u} = -\nabla P + \mu (\nabla \boldsymbol{u} + (\nabla \boldsymbol{u})^T)$	(4)
Work done by pressure changes	$Q_p = -\frac{1}{\rho}\frac{\partial \rho}{\partial T} T (\boldsymbol{u} \cdot \nabla P)$	(2)	Continuity equation	$\rho \nabla \boldsymbol{u} = 0$	(5)
Viscous dissipation effect	$Q_{vd} = \boldsymbol{\tau} : \nabla \boldsymbol{u}$	(3)			

Boundary conditions

To determine the flow field generated by the twin screw motion, a rotation velocity was equally applied to both screws. Velocity was changed at 100 RPM, 250 RPM and 500 RPM while the extrusion chamber was kept relatively fixed. For the flow field, an open boundary condition was applied at the inlet of the extruder chamber, while atmospheric pressure was applied at the outlet of the cooled slot die. Furthermore no-slip condition was used along the walls of the extruder chamber. For heat transfer equation, inlet boundary condition was applied with a temperature equal to 25°C, while assigning temperatures of 25°C, 25°C, 40°C, 60°C, 80°C, 100°C, 120°C, 130°C, 110°C respectively at each zone from 1 to 9. Temperature at cooling slot die was set at 70°C to have product temperature below 75°C (Xiaonan et al., 2024).

Material properties

The geometry block was assumed to be the extruder chamber and cooling slot die completely filled with soy dough, having 65 % w/w moisture content. This moisture content was previously used (Lin et al., 2000) to extrude in a lab-scale HME process. Physical properties like specific heat C_p (J kg^{-1} K^{-1}), thermal conductivity k (W m^{-1} K^{-1}) and thermal diffusivity α (m^2/s) and density ρ (kg/m^3) were obtained by literature (Högg and Cornelia, 2023) as a function of temperature, except for the density. Viscosity, a key property, strongly depends on the fluid dynamics and temperature and this was accounted using parameters, power n and consistency coefficient m (Pa s), according to 'Power Law' model (Dashu et al., 2024).

Discretization, mesh and convergence

A second order (P2) velocity and first order (P1) pressure configuration were selected for the discretization of the fluid variables to meet the 'inf-sup' (LBB) condition (Arnold et al., 1984) and achieve a smooth and high accuracy velocity field. Mesh convergence studies were performed to ensure that the results were independent of mesh resolution. With this aim, the influence of meshing a fluid flow field and heat transfer solution, coupled with rotor moving mesh, was analyzed using the highest screw speed (500 RPM). Maximum element size and minimum element size were set by changing the size mesh parameter (SM [m]) using the parametric sweep

analysis. The outward mass flow rate (Eq(6)) and the viscous dissipation (Eq(3)) were calculated and used to evaluate the mesh influence.

$$\dot{m}=\rho \int \mathbf{u}\, dS \quad (6)$$

According to literature (Ali G., 2013), volumetric flow rates fluctuation between 1 to 8 % should be considered to be indicating that the mesh dependency is negligible. The results found that the calculated mass flow rate changed between 10.596 to 12.971 kg/h. The presented results always corresponded to the highest mesh density value shown in Table 2.

Table 2 Mesh dependency analysis at different number of cells

Case	Numbers of degrees of freedom [unit]	Mass flow rate [kg/h]	Error MFR [%]	Total viscous dissipation [W]	Error TVD [%]
Case 1	$1.88 \cdot 10^6$	12.971	/	473	/
Case 2	$1.23 \cdot 10^6$	12.191	6	478	1
Case 3	$0.88 \cdot 10^6$	11.164	8.4	482	0.8

Pumping efficiency

The ratio between the total throughput and theoretical throughput based on its C-shaped chamber volume is called *pumping efficiency* (Ali G., 2013). This factor multiplied the theoretical throughput gives the total throughput. The theoretical throughput Q_{th} was calculated as reported in Eq(7) (Ali G., 2013).

$$Q_{th}=2\, N\, V_c\, \rho \quad (7)$$

The C-shaped chamber volume can be calculated by subtracting the volume of a given length of screw from the same length of the empty barrel. The volume V_1 of one side of the barrel bore over one flight lead was calculated as in Eq(8).

$$V_1=\left\{\left(\pi-\frac{\alpha}{2}\right) R^2+\left(R-\frac{H}{2}\right)\sqrt{(RH-H^4)}\right\} S \quad (8)$$

These geometrical parameters are shown in Figure 2.

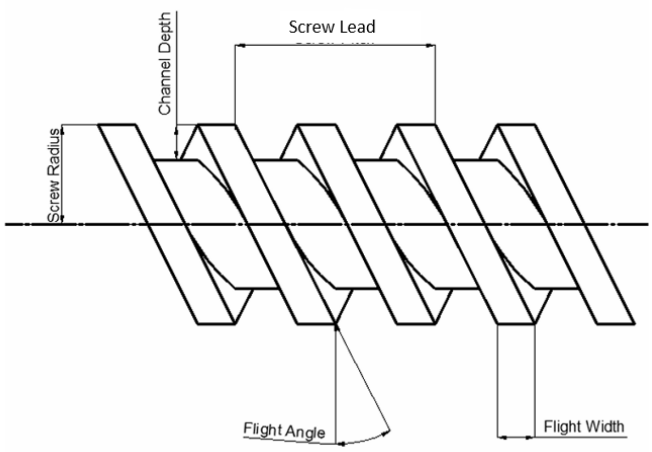

Figure 2 Geometrical parameters for simple model of theoretical output

α is defined as the overlapping angle (rad) and was calculated as in Eq(9).

$$\alpha=2\tan^{-1}\left(\frac{\sqrt{R^2-\frac{H^2}{4}}}{R-\frac{H}{2}}\right) \quad (9)$$

The volume V_2 of the screw root over one pinch length was calculated as in Eq(10).

$$V_2=S\pi(R-H)^2 \quad (10)$$

The volume V_3, of one screw flight, was calculated as in Eq(11).

$$V_3=2\pi\left[\left(RH-\frac{H^2}{2}\right) W_f+\left(RH^2-\frac{2}{3}H^3\right)\tan(\theta)\right] \quad (11)$$

The total volume of C-shaped chamber was calculated as in Eq(12).

$$V_c = \frac{V_1 - V_2 - iV_3}{i} \quad (12)$$

Values of the up mentioned variables were calculated and reported in Table 3.

Table 3 Geometrical parameters and mass flow rate results at different screw speed

ρ	Soy dough density	[kg/m^3]	1120.00
i	Number of screw flight	[-]	2
R	Screw radius	[mm]	6.70
H	Channel depth	[mm]	1.90
S	Screw lead length	[mm]	12.00
W_f	Flight width	[mm]	0.53
θ	Flight angle	[°]	16.00
Q_{th}	Theoretical mass flow rate (no leakage)	100/250/500 RPM [kg/h]	3.13/7.82/15.62

Dispersive mixing behavior

Ali G. (2013) mentioned that evaluating the dispersive mixing parameter of a twin screw extruder was a valuable measure. The dispersive mixing parameter λ is defined by Eq(8) (Manas-Zloczower et al., 1989).

$$\lambda = \frac{|\dot{\gamma}|}{|\dot{\gamma}| + |\omega|} \quad (8)$$

λ quantifies the elongational and rotational flow which are often thought to be more strongly relevant to dispersive mixing compared to shear. It has a value between 0 and 1, where λ = 0 indicates pure rotation while λ = 1 indicates pure elongation and λ = 0.5 corresponds to simple shear flow.

2.3 Numerical solution

The CFD and heat transfer simulation were carried out using the commercial solver Comsol Multiphysics 6.2. Computations were carried out on a PC with Intel® Core™ i7-7700HQ CPU @ 2.80 GHz 2.81 GHz, RAM 16 GB, NVIDIA GeForce GTX 1050 12228 MB 640 CUDA Core.

3. Results

3.1 Axial velocities - effect of screw lead length and tip width

The screw profile is repeated for each lead length in feeding, transport and extrusion zones. Consequently, only axial velocities distribution from 0° to 135 ° planes are plotted. Axial velocities distribution in planes are shown at screw speed equal to 500 RPM for feeding zone in Figure 3, for transport zone in Figure 4, and for extrusion zone in Figure 5. Figure 3 for feeding zone shows highest values of axial velocity occurred at 135° plane and before the converging section of the intermeshing region. While most negative values are located at 45° plane inside the intermeshing region. These results are in according with the literature (Ali G., 2013). The symmetry along screws' inter-axis generates negative values of axial velocities. Similar behaviors are shown in Figure 4 and Figure 5 suggesting that there is no dependence on the lead length and tip width. However, along transport and extrusions zone negative values of velocities are less pronounced, suggesting a favorable lower material leakage or backflow. This result potentially affects material residence time and mixing efficiency during extrusion process.

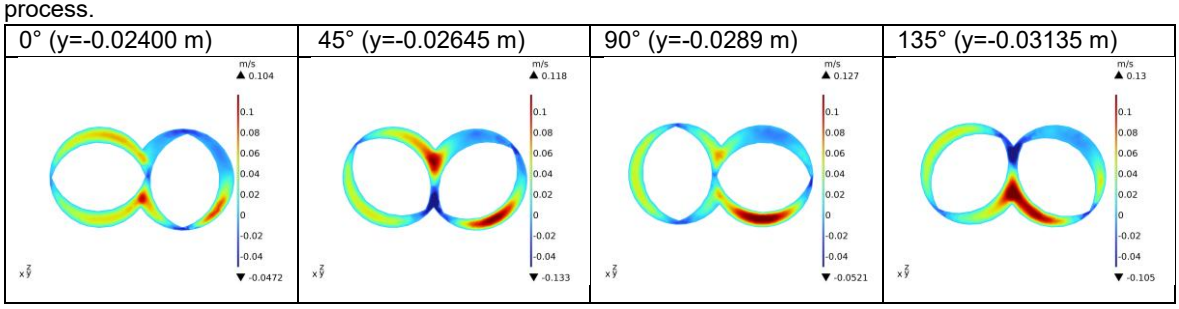

Figure 3 Axial velocities distribution at 500 RPM in feeding zone at planes from 0° to 135° (20 mm lead)

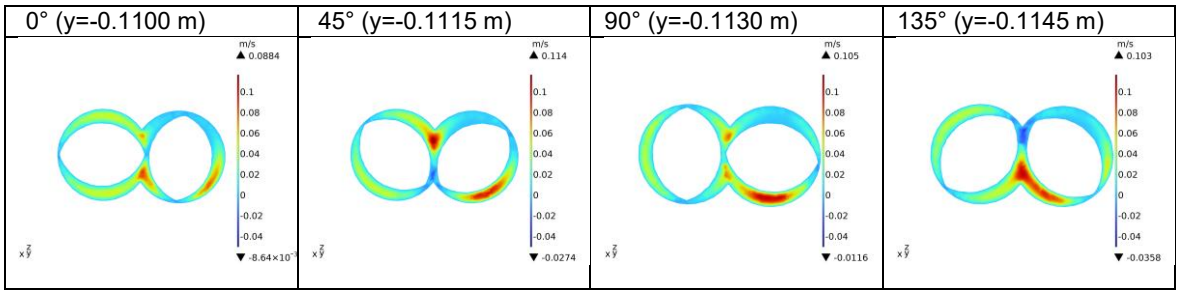

Figure 4 Axial velocities distribution 500 RPM in transport zone at planes from 0 to 135° (12 mm lead)

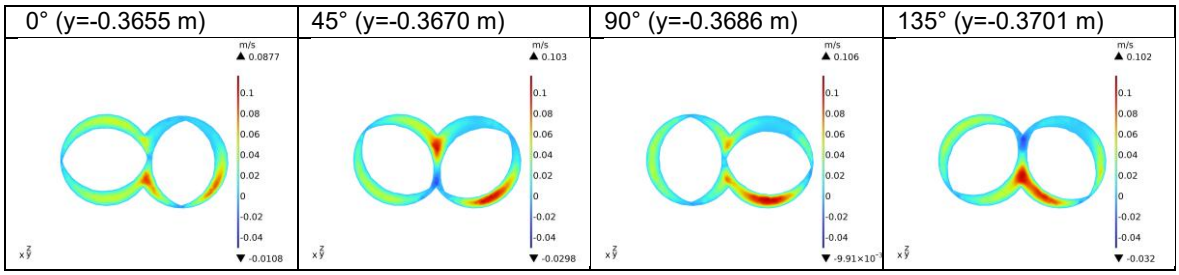

Figure 5 Axial velocity distribution at 500 RPM in extrusion zone from 0 to 135° planes (12 mm lead)

3.2 Pumping behaviour – effect of screw speed

The pumping efficiency was calculated for each screw speed. The results are shown in Table 4. An increase in screw speed modified slightly the pumping efficiency (0.77-0.83) suggesting that screw speed affects the theoretical flow rate and total flow rate at the same degree according to the literature (Ali G., 2013). This suggests that leakage flows and other secondary effects had a negligible impact on throughput.

Table 4 Calculation of total mass flow rate and theoretical mass flow rate

Q_{ac}	Total mass flow rate	100/250/500 RPM	[kg/h]	2.40/6.29/12.97
η	Pumping efficiency	100/250/500 RPM	/	0.77/0.80/0.83

3.3 Dispersive mixing behaviour - effect of screw speed

Quantification of mixing is challenging in extrusion processing. To evaluate the dispersive mixing efficiency the dispersive mixing parameter λ was used in this analysis in the mixing zone, its definition is reported in Eq(8). |γ|, the magnitude of the rate of strain tensor, and |ω|, the magnitude of the rate of vorticity tensor, were calculated by Comsol Multiphysics and results are shown in Table 5. Results show that no influence of screw speed on dispersive mixing parameter occurred (0.451-0.454). On the basis of previous mixing parameter classification, obtained values suggest a simple shear flow behavior in the mixing zone.

Table 5 Dispersive mixing parameter evaluated in the mixing zone at different screw speed

|γ|	Magnitude of the rate of strain tensor	100/250/500 RPM	[1/s]	60/151/300
|ω|	Magnitude of the rate of vorticity tensor	100/250/500 RPM	[1/s]	72/180/365
λ	Dispersive mixing parameter	100/250/500 RPM	/	0.454/0.456/0.451

4. Conclusions

Axial velocity distribution showed that the highest velocities occurred in the intermeshing regions of the screws, promoting material transport, while localized negative velocities were observed in specific planes. These variations suggest that backflow and recirculation zones are influenced by screw geometry, potentially affecting

material residence time and mixing efficiency with a potential impact on fiber alignment and protein structuring during texturization process. Pumping efficiency remained relatively stable (0.77–0.83) across different screw speeds, indicating that the total mass flow rate increased proportionally with the theoretical value predicted by an analytical model. This suggests that leakage flows and other secondary effects had a negligible impact on throughput, confirming the reliability of theoretical predictions for process scaling and optimization. The dispersive mixing parameter exhibited minimal variation (0.451–0.456) across different screw speeds, indicating that the mixing zone predominantly induced simple shear flow. This behaviour suggests that screw speed does not significantly alter dispersive mixing efficiency under the tested conditions. This flow type is beneficial for partial protein denaturation and molecular realignment, facilitating the formation of structured protein networks. Maintaining a controlled shear environment prevents excessive fragmentation, ensuring the development of elongated protein fibers essential for meat analog texture. The study offers useful insights for optimizing extrusion parameters, enhancing process control, and improving the consistency of protein structuring in meat analog production.

Nomenclature

ρ – material density, kg/m^{3}Cp – specific heat capacity of soy dough, J/(kg·K)
k – thermal conductivity of soy dough, W/(m·K)
T – temperature, K
u – velocity field, m/s
Q_p – work done by pressure changes, W/m^3
Q_{vd} – viscous dissipation in the fluid, W/m^3
P – pressure, Pa
$\boldsymbol{\tau}$ – viscous stress tensor, Pa
Q_{th} – theoretical mass flow rate, kg/h
Q_{ac} – total mass flow rate, kg/h
$|\gamma|$ - magnitude of the rate of strain tensor, 1/s
$|\omega|$ - magnitude of the rate of vorticity tensor, 1/s
μ – non-newtonian viscosity, Pa·s
N – screw rotation speed, 1/s
V_c – C-shaped volume chamber, m^3
η – pumping efficiency, -
S – screw lead length, m
R - screw radius, m
H – channel depth, m
W_f – flight width, m
α – overlapping angle, °
θ – flight angle, °
y – axis direction, m

References

Ali G. (2013). Modelling of counter rotating twin screw extrusion, Master Thesis, Mc Master University, 1-145. Copyright by Ali Goger, August 2013, Hamilton, Ontario.

Arnold, D.N., Babuˇska, I., Osborn, J., 1984. Finite element methods: Principles for their selection. Comput. Methods Appl. Mech. Eng. 45, 57–96.

Dashu L., Tianqui Z., Fei G., Chengyi Z., Dongyu S., Yutong G and Min W.(2024). The study of numerical simulation and texture of soybean protein based on high moisture extrusion with different screw elements. Innovative Food Science and Emerging Technologies, 92, 103560.

Datta A., Nicolai B., Vitrac O., Verboven P., Erdogdu F., Marra F., Sarghini F., Koh C. (2022). Computer-aided food engineering. Nature Food, Nov;3(11):894-904.

Högg E. and Cornelia R. (2023). Towards a better understanding of Texturization during High-Moisture Extrusion. Foods, 12, 2283.

Hong W., Frans W.J.V., Wei Z., Tomasz P.C., Longteng Z., Birthe M.J., R.L. (2022). Differences in physicochemical properties of high-moisture extrudates prepared from soy and pea protein isolates. Food Hydrocolloids, 128, 107540.

Kousemaker, T. M., Druetta, P., Picchioni, F., & Vakis, A. I. (2024). Modelling supercritical CO2 flow in a co-rotating twin screw extruder using the level-set method. Chemical Engineering Research and Design, 205, 569-577.

Lin. S., Huff H.E. and Hsieh F. (2000). Texture and Chemical Characteristics of Soy Protein Meat Analog Extruded at High Moisture. Journal of Food Science, Vol.65, No.2.

Manas-Zloczower I. and Feke D.L.(1989). Int. Polym. Proc., IV, 3-8.

Verboven, P., Defraeye, T., Datta, A. K. & Nicolai, B. (2020). Digital twins of food process operations: the next step for food process models? Curr. Opin. Food Sci. 35, 79–87.

Xiaonan S., Tianyi Z., Xin Z., Lianzhou J. (2024). High-Moisture Extrusion of Plant Proteins: Fundamentals of Texturization and Applications. Annu. Rev. Food Sci. Technol., 15:125-49.